the monomeric [Ni(tsb)] molecules associate in solution, it is reversible via intermonomer bonds, rather than via the two ends of tsb ligands acting as bidentates on two different metals.

Although [Cu(cbpO)], with its weak Cu–O ether linkage, can model the behavior of four-coordinated Cu^{II} and Ni^{II} complexes of type **3** ligands, it is unlikely that [Ni(cbpO)] would be equally appropriate. Comparison of complexes with ligand **1** indicates a generally much stronger M–X bonding in the Ni^{II} complexes than in their Cu^{II} analogues. This difference in structural behavior between d^8 and d^9 (and the equally dramatic difference between d^7 and d^9) is readily explained in terms of the crystal field stabilizing energies (CFSE) of these electronic configurations in various ligand environments.[7,11]

Magnetic Moments. The observed value of 1.80 μ_B for [Cu(cbpO)] is typical for Cu(II) in an orbitally nondegenerate ground state and corresponds to an effective *g* value of 2.08. In [Co(cbpO)], the moment, 4.78 μ_B, indicates high-spin d^7, which is the only result compatible with the observed trigonal-bipyramidal structure. Five-coordinated low-spin d^7 would gain considerable CFSE by a tetragonal distortion which elongates the M–X bond, as would d^9. This strong stabilization does not apply for high-spin d^7, and electrostatic repulsion is important in forcing the observed trigonal-bipyramidal environment of [Co(cbpO)].

Acknowledgment. Support received for instrumentation under NSF Grant Gp-41679 is gratefully acknowledged.

Registry No. Cu(cbpO), 76136-67-9; Co(cbpO), 76136-66-8; 5-chloro-2-hydroxybenzophenone, 85-19-8; bis(3-aminopropyl) ether, 2157-24-6.

Supplementary Material Available: Tables of observed and calculated structure factors and calculated least-squares planes (24 pages). Ordering information is given on any current masthead page.

---

(36) Kirson, B.; Sechter, H. *Bull. Soc. Chim. Fr.* **1965**, 2743.

Contribution from the Departments of Chemistry, University of Virginia, Charlottesville, Virginia 22901,
and William Marsh Rice University, Houston, Texas 77001

Electronic and Molecular Structure of Variable-Spin Metal Complexes. Spin State Dependent Crystal and Molecular Structures of $[Fe^{III}(5\text{-}OCH_3Salmeen)_2]PF_6$ ($S = {}^5/_2$), $[Fe^{III}(3\text{-}OCH_3Salmeen)_2]PF_6$ ($S = {}^1/_2$), and $[Fe^{III}(5\text{-}NO_2Salmeen)_2]PF_6$ ($S = {}^1/_2$)

P. GREIG SIM,[1a] EKK SINN,*[1a] RANDALL H. PETTY,[1b] CONNIE L. MERRILL,[1b] and LON J. WILSON*[1b]

Received August 13, 1980

Spin state dependent crystal structure determinations of three six-coordinate $3d^5$ complexes of the $[Fe^{III}(X\text{-}Salmeen)_2]PF_6$ series of spin-equilibrium compounds (X = 5-OCH_3, 3-OCH_3, and 5-NO_2) are reported. At room temperature, the 5-OCH_3 derivative is a $S = {}^5/_2$ high-spin species ($\mu_{eff}{}^{295} = 5.75\ \mu_B$), whereas the 5-$NO_2$ ($\mu_{eff}{}^{295} = 2.58\ \mu_B$) and 3-$OCH_3$ ($\mu_{eff}{}^{298} = 3.20\ \mu_B$) derivatives are at or near the $S = {}^1/_2$ low-spin extreme. The structural determinations reveal that the three $[Fe^{III}(X\text{-}Salmeen)_2]^+$ cations possess the same general structure with an N_4O_2 donor atom set from two tridentate X–Salmeen ligands forming a distorted octahedron about the metal ion. In each case the terminal oxygen atoms occupy cis positions and the remaining four nitrogen atoms (two cis amines and two trans imines) complete the coordination sphere. The fine structural details for the three compounds reveal significant differences in the metal atom environments which can be largely attributed to the differing $S = {}^5/_2$ and $S = {}^1/_2$ spin states. For the $S = {}^5/_2$ complex, the average Fe–ligand bond length (δ_{av}) is longer by about 0.12 Å relative to the two $S = {}^1/_2$ cases, but the difference is not uniform: the Fe–N bonds vary far more [δ(amino) = 0.16 Å; δ(imino) = 0.16 Å] than the Fe–O bonds (δ = 0.02 Å). The spin state dependent structural changes observed for the $[Fe^{III}(X\text{-}Salmeen)_2]^+$ spin-equilibrium cations are compared to results previously reported for the electronically and structurally related hexadentate cations $[Fe^{III}(Sal)_2trien]^+$ and $[Fe^{III}(Acac)_2trien]^+$, for which δ_{av} is also 0.12–0.13 Å. In addition, variable-spin structural information now available for a variety of other $3d^5$ (and $3d^6$) spin-equilibrium compounds is also discussed in the context of the present results for the $[Fe^{III}(XSalmeen)_2]^+$ series of complexes. Crystal data for $[Fe^{III}(5\text{-}OCH_3Salmeen)_2]PF_6$: $FePF_6O_4N_4C_{22}H_{30}$, space group *Pbca*, $Z = 8$, $a = 10.263$ (3) Å, $b = 19.696$ (6) Å, $c = 26.768$ (6) Å, $V = 5411$ Å^3, $R = 5.1\%$ for 2712 reflections. Crystal data for $[Fe^{III}(3\text{-}OCH_3Salmeen)_2]PF_6$: $FePF_6O_4N_4C_{22}H_{30}$, space group $P2_1/c$, $Z = 4$, $a = 11.627$ (2) Å, $b = 10.412$ (5) Å, $c = 21.632$ (9) Å, $\beta = 92.62$ (2)°, $V = 2616$ Å^3, $R = 6.3\%$ for 2341 reflections. Crystal data for $[Fe^{III}(5\text{-}NO_2Salmeen)_2]PF_6$: $FePF_6O_6N_6C_{20}H_{24}$, space group *Pbcn*, $Z = 4$, $a = 12.609$ (7) Å, $b = 12.927$ (4) Å, $c = 16.122$ (2) Å, $V = 2628$ Å^3, $R = 4.7\%$ for 1648 reflections.

Introduction

The high-spin and low-spin magnetic isomeric forms of spin-equilibrium transition-metal complexes are now well-known to possess different average metal–ligand bond lengths, with the bonds of the low-spin form being significantly shorter.[2-12] Accordingly, spin-equilibrium species with ligands having bulky substituents and significient *inter*ligand steric interactions have a marked tendency to produce elongated metal–ligand bonds associated with the high-spin configuration. In addition, since such complexes lie near the (high spin) ⇄ (low spin) crossover, environmental effects such as changes in temperature,[13-16] pressure,[17,18] counterions,[9,19-21] occluded

---

(1) (a) University of Virginia. (b) William Marsh Rice University.

(2) König, E.; Watson, K. J. *Chem. Phys. Lett.* **1970**, *6*, 457.

(3) Leipoldt, J. G.; Coppens, P. *Inorg. Chem.* **1973**, *12*, 2269.

(4) Hoskins, B. F.; Pannan, C. G. *Inorg. Nucl. Chem. Lett.* **1975**, *11*, 409.

(5) Hoselton, M. A.; Wilson, L. J.; Drago, R. S *J. Am. Chem. Soc.* **1975**, *97*, 1722.

(6) Wilson, L. J.; Georges, D.; Hoselton, M. A. *Inorg. Chem.* **1975**, *14*, 2968.

(7) Cukauskas, E. J.; Deaver, B. S., Jr; Sinn, E. *J. Chem. Phys.* **1977**, *67*, 1257.

(8) Greenaway, A. M.; Sinn, E. *J. Am. Chem. Soc.* **1978**, *100*, 8080.

(9) Sinn, E.; Sim, P. G.; Dose, E. V.; Tweedle, M. F.; Wilson, L. J. *J. Am. Chem. Soc.* **1978**, *100*, 3375.

(10) Katz, B. A.; Strouse, C. E. *J. Am. Chem. Soc.* **1979**, *101*, 6214.

(11) Katz, B. A.; Strouse, C. E. *Inorg. Chem.* **1980**, *19*, 658.

(12) Oliver, J. D.; Mullica, D. F.; Hutchinson, B. B.; Milligan, W. O. *Inorg. Chem.* **1980**, *19*, 165.

(13) Sylva, R. N.; Goodwin, H. A. *Aust. J. Chem.* **1969**, *21*, 83.

(14) Harris, C. M.; Patil, H. R. H.; Sinn, E. *Inorg. Chem.* **1969**, *8*, 101.

(15) Harris, C. M.; Kokot, S.; Patil, H. R. H.; Sinn, E.; Wong, *H. Aust. J. Chem.* **1972**, *25*, 1631.

(16) Halbert, E. J.; Harris, C. M.; Sinn, E.; Sutton, G. J. *Aust. J. Chem.* **1973**, *26*, 951.

0020-1669/81/1320-1213$01.25/0

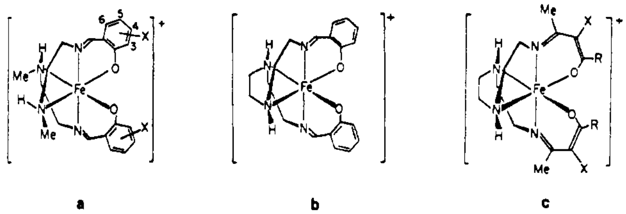

Figure 1. General structures for the variable-spin (a) $[Fe^{III}(X\text{-}Salmeen)_2]^+$, (b) $[Fe^{III}(Sal)_2trien]^+$, and (c) $[Fe^{III}(AcacX)_2trien]^+$ (with R = Me) cations.

solvent molecules,[8,9,19,22] and even geometrical isomerism[10] can also be influential in determining the final distribution of the spin isomers. Since the magnitude and pattern of metal–ligand bond distance changes accompanying spin conversion are of fundamental interest in structural transition-metal chemistry,[23] metallophotochemistry,[24] and metalloprotein chemistry,[25] there is a decided need for a continuing documentation of the molecular structural changes which accompany the phenomenon. This paper reports the correlation between molecular structure and spin state for three members of the $[Fe^{III}(X\text{-}Salmeen)_2]^+$ family of $(S = {}^5/_2) \rightleftarrows (S = {}^1/_2)$ spin-equilibrium complexes which were reported earlier.[26] Generalized structures for these pseudooctahedral, bis tridentate $[Fe^{III}(X\text{-}Salmeen)_2]^+$ cations with X = 3-OCH_3, 5-OCH_3, and 5-NO_2 are shown in Figure 1a. Salmeen is the Schiff base condensate of salicylaldehyde and *N*-methylethylenediamine. At room temperature, the 5-OCH_3 derivative, as the PF_6^- salt, is a high-spin $S = {}^5/_2$ species ($\mu_{eff}{}^{295} = 5.75\ \mu_B$), whereas the 3-$OCH_3$ and 5-NO_2 derivatives are both more nearly $S = {}^1/_2$ low-spin compounds ($\mu_{eff}{}^{298} = 3.20\ \mu_B$ and $\mu_{eff}{}^{295} = 2.58\ \mu_B$, respectively).[26]

While a structural/spin state correlation for the present $[Fe^{III}(X\text{-}Salmeen)_2]^+$ complexes is probably best considered in light of parallel information available for the structurally related $[Fe^{III}(Sal)_2trien]^+$ and $[Fe^{III}(AcacX)_2trien]^+$ compounds of Figure 1b and 1c,[9,20,21] a growing body of similar information is also now available for several other pseudooctahedral iron(III)[3,4,8] and iron(II)[2,5–7,10–12] systems undergoing spin equilibria. As in the present study, most of this spin state dependent structural information has been generated by X-ray crystallographic studies at room temperature, with the notable exceptions being for the $[Fe^{II}(2,2\text{-}bpy)_2(NCS)_2]^{2+}$, $[Fe^{III}(dtc)_3]$, and $[Fe^{II}(2\text{-}pic)_3]^{2+}$ complexes where variable-temperature crystallography has been used to special advantage.[2,3,10] In the most complete of these variable-temperature studies, Katz and Strouse[10] were able to resolve the structures of the two different spin isomers in the same crystal lattice containing the $[Fe^{II}(2\text{-}pic)_3]^{2+}$ cation.

Experimental Section

Syntheses. Syntheses of the compounds were performed as previously described.[26] Suitable crystals of the X = 5-OCH_3 derivative were obtained from a saturated methanol solution into which heptane was slowly allowed to diffuse over several days. The remaining two compounds were crystallized by slow evaporation of a solution of the compound in a 1:1 CH_2Cl_2–heptane mixture.

Crystal Data for $[Fe^{III}(3\text{-}OCH_3Salmeen)_2]PF_6$: $FePF_6O_4N_4C_{22}H_{30}$, mol wt 615, space group $P2_4/c$, $Z = 4$, $a = 11.627$ (2) Å, $b = 10.412$ (5) Å, $c = 21.632$ (9) Å, $\beta = 92.62$ (2)°, $V = 2616$ Å^3, $\rho_{calcd} = 1.56$ g cm^{-3}, $\rho_{obsd} = 1.56$ g cm^{-3}, μ(Mo Kα) = 7.4 cm^{-1}; crystal dimensions (distances in mm of faces from centroid) (100) 0.08, $(\bar{1}00)$ 0.08, (010) 0.425, $(0\bar{1}0)$ 0.425, (001) 0.095, $(00\bar{1})$ 0.095; maximum and minimum transmission coefficients 0.96, 0.93.

Crystal Data for $[Fe^{III}(5\text{-}NO_2Salmeen)_2]PF_6$: $FePF_6O_6N_6C_{20}H_{24}$, mol wt 645, space group *Pbcn*, $Z = 4$, $a = 12.609$ (7) Å, $b = 12.927$ (4) Å, $c = 16.122$ (2) Å, $V = 2628$ Å^3, $\rho_{calcd} = 1.63$ g cm^{-3}, $\rho_{obsd} = 1.61$ g cm^{-3}, μ(Mo Kα) = 7.5 cm^{-1}; crystal dimensions (mm from centroid) (111) 0.31, $(\bar{1}\bar{1}\bar{1})$ 0.31, $(\bar{1}11)$ 0.28, $(1\bar{1}\bar{1})$ 0.28, $(1\bar{1}1)$ 0.325, $(\bar{1}1\bar{1})$ 0.325, $(\bar{1}\bar{1}1)$ 0.31, (001) 0.185, $(0\bar{1}\bar{5})$ 0.15, maximum and minimum transmission coefficients 0.73, 0.50.

Crystal Data for $[Fe^{III}(5\text{-}OCH_3Salmeen)_2]PF_6$: $FePF_6O_4N_4C_{22}H_{30}$, mol wt 615, space group *Pbca*, $Z = 8$, $a = 10.263$ (3) Å, $b = 19.696$ (6) Å, $c = 26.768$ (6) Å, $V = 5411$ Å^3, $\rho_{calcd} = 1.511$ g cm^{-3}, $\rho_{obsd} = 1.52$ g cm^{-3}, μ(Mo Kα) = 7.2 cm^{-1}; crystal dimensions (mm from centroid), (100) 0.425, $(\bar{1}00)$ 0.425, (010) 0.08, $(0\bar{1}0)$ 0.08, (001) 0.23, $(00\bar{1})$ 0.23; maximum and minimum transmission coefficients 0.92, 0.88.

For each crystal, the Enraf-Nonius program SEARCH was used to obtain 25 accurately centered reflections which were then used in the program INDEX to obtain approximate cell dimensions and an orientation matrix for data collection. Refined cell dimensions and their estimated standard deviations were obtained from least-squares refinement of 28 accurately centered reflections. The mosaicity of each crystal was estimated by the ω-scan technique and judged to be satisfactory.

Collection and Reduction of Data. Diffraction data were collected at 292 K on an Enraf-Nonius four-circle CAD-4 diffractometer controlled by a PDP8/M computer, using Mo Kα radiation from a highly oriented graphite crystal monochromator. The θ–2θ scan technique was used to record the intensities for all nonequivalent reflections for which $1° < 2\theta < 46°$ for $[Fe^{III}(3\text{-}OCH_3Salmeen)_2]PF_6$, $1° < 2\theta < 46°$ for $[Fe^{III}(5\text{-}NO_2Salmeen)_2]PF_6$, and $1° < 2\theta < 48°$ for $[Fe^{III}(5\text{-}OCH_3Salmeen)_2]PF_6$. Scan widths (SW) were calculated from the formula SW = $A + B \tan \theta$, where A is estimated from the mosaicity of the crystal and B allows for the increase in width of peak due to Kα_1–Kα_2 splitting. The values of A and B were 0.60 and 0.35°, 0.60 and 0.35°, and 0.60 and 0.30° for the three complexes, respectively. The calculated scan angle is extended at each side by 25% for background determination (BG1 and BG2). The net count is then calculated as NC = TOT − 2(BG1 + BG2), where TOT is the integrated peak intensity. Reflection data were considered insignificant if intensities registered less than 10 counts above background on a rapid prescan, such reflections being rejected automatically by the computer.

The intensities of four standard reflections, monitored for each crystal at 100 reflection intervals, showed no greater fluctuations during the data collection than those expected from Poisson statistics. The raw intensity data were corrected for Lorentz–polarization effects (including the polarization effect of the crystal monochromator) and then for absorption. After the intensities of equivalent reflections were averaged, the data were reduced to 3260 independent intensities for $[Fe^{III}(3\text{-}OCH_3Salmeen)_2]PF_6$, 1900 for $[Fe^{III}(NO_2Salmeen)_2]PF_6$, and 4042 for $[Fe^{III}(5\text{-}OCH_3Salmeen)_2]PF_6$, of which 2341, 1648, and 2712 for the three compounds, respectively, had $F_o^2 > 3\sigma(F_o^2)$, where $\sigma(F_o^2)$ was estimated from counting statistics.[27] These data were used in the final refinement of the structural parameters.

Determination and Refinement of the Structures. Full-matrix least-squares refinement was based on F, and the function minimized was $\sum w(|F_o| - |F_c|)^2$. The weights w were taken as $[2F_o/\sigma(F_o^2)]^2$, where $|F_o|$ and $|F_c|$ are the observed and calculated structure factor amplitudes. The atomic scattering factors for nonhydrogen atoms were taken from Cromer and Waber[28] and those for hydrogen from Stewart et al.[29] The effects of anomalous dispersion for all nonhy-

---

(17) See for example: Fung, S. C.; Drickamer, H. G. *J. Chem. Phys.* **1969**, *51*, 4350, 4360.

(18) Ewald, A. H.; Martin, R. L.; Sinn, E.; White, A. H. *Inorg. Chem.* **1969**, *8*, 1837.

(19) Harris, C. M.; Lockyer, T. N.; Martin, R. L.; Patil, H. R. H.; Sinn, E.; Stewart, J. M. *Aust. J. Chem.* **1969**, *22*, 2105.

(20) Tweedle, M. F.; Wilson, L. J. *J. Am. Chem. Soc.* **1976**, *98*, 4824.

(21) Dose, E. V.; Murphy, K. M. M.; Wilson, L. J. *Inorg. Chem.* **1976**, *15*, 2622.

(22) Cukauskas, E. J.; Deaver B. S., Jr.; Sinn, E. *J. Chem. Phys.* **1977**, *67*, 1257.

(23) References 2–12 and references therein.

(24) See for example: Adamson, A. W. *Adv. Chem. Ser.* **1976**, *No. 150*, 128–148.

(25) See for example: Dose, E. V.; Tweedle, M. F.; Wilson, L. J.; Sutin, N. *J. Am. Chem. Soc.* **1977**, *99*, 3886.

(26) Petty, R. H.; Dose, E. V.; Tweedle, M. F.; Wilson, L. J. *Inorg. Chem.* **1978**, *17*, 1064.

(27) Corfield, P. W. R.; Doedens, R. J.; Ibers, J. A. *Inorg. Chem.* **1967**, *6*, 197.

(28) Cromer, D. T.; Waber, J. T. "International Tables for X-ray Crystallography"; Kynoch Press: Birmingham, England, 1974; Vol. IV.

(29) Stewart, R. F.; Davidson, E. R.; Simpson, W. T. *J. Chem. Phys.* **1965**, *42*, 3175.

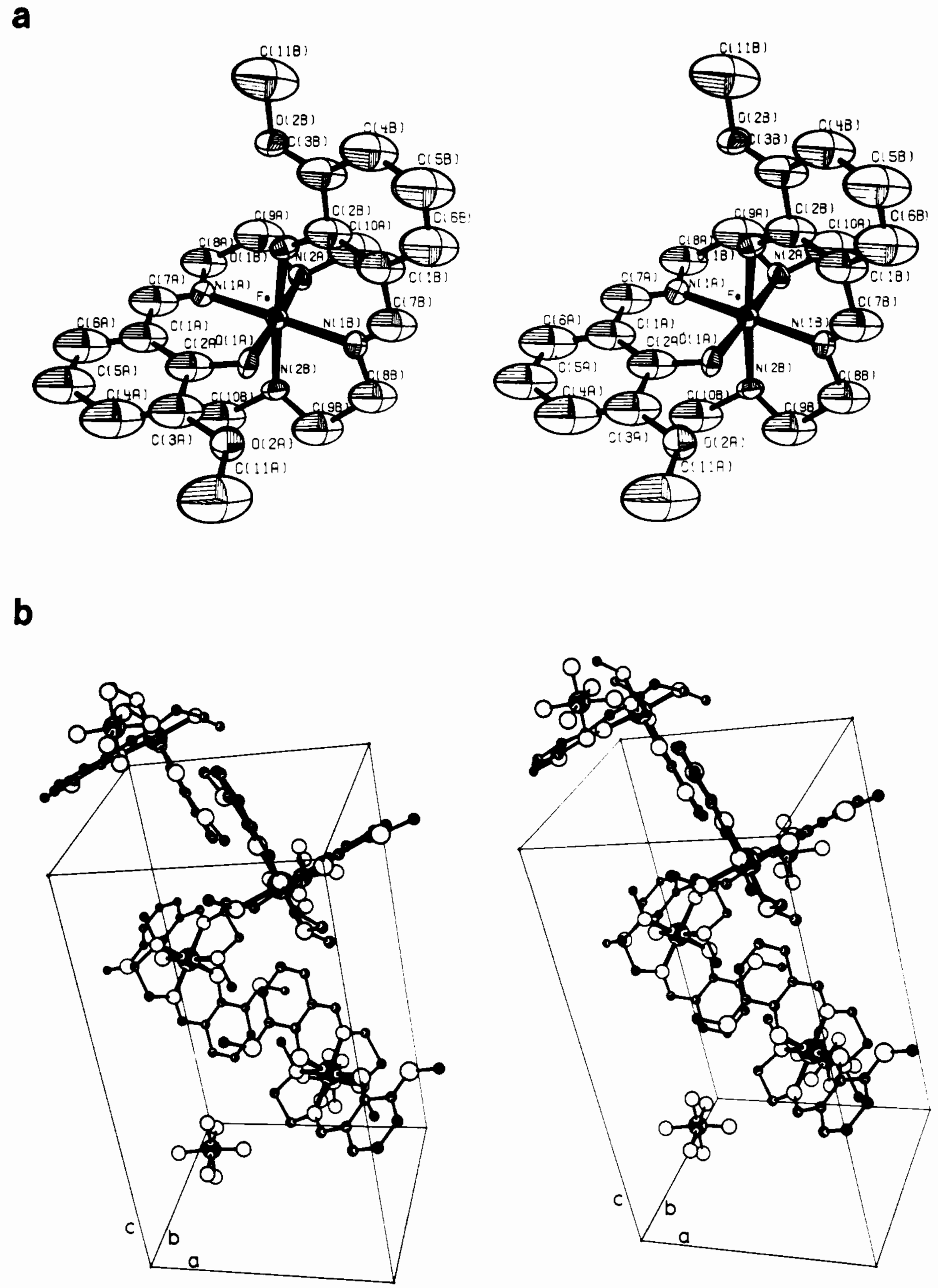

Figure 2. (a) Stereopair view of the $[Fe^{III}(3\text{-}OCH_3Salmeen)_2]^+$ cation in $[Fe^{III}(3\text{-}OCH_3Salmeen)_2]PF_6$. (b) Stereopair view of the molecular packing for the $[Fe^{III}(3\text{-}OCH_3Salmeen)_2]PF_6$ salt.

drogen atoms were included in F_c with use of the values of Cromer and Ibers[30] for $\Delta f'$ and $\Delta f''$. Agreement factors are defined as $R = \sum||F_o| - |F_c||/\sum|F_o|$ and $R_w = (\sum w(|F_o| - |F_c|)^2/\sum w|F_o|^2)^{1/2}$.

In each case the positions of the iron and some of the ligand atoms were determined from three-dimensional Patterson functions calculated from all intensity data. The intensity data were phased sufficiently well by these positional coordinates to permit location of the remaining nonhydrogen atoms from Fourier syntheses. In the case of $[Fe^{III}(5\text{-}NO_2Salmeen)_2]PF_6$, the space group, the unit cell size, and the Patterson map suggested that both the iron and phosphorus atoms should lie on a twofold symmetry axis. Solution of the structure confirmed this hypothesis. In the case of $[Fe^{III}(3\text{-}OCH_3Salmeen)_2]PF_6$ the PF_6 group was found to be positionally disordered, by an approximate 45° rotation about one F–P–F axis (F(1′)–P–F(2)) of the octahedral anion. Thus, atoms, P, F(1), and F(2) were refined with occupancy factors of 1.0, while values of 0.60 were used for F(3)–F(6) and 0.40 for F(3′)–F(6′).

Anisotropic temperature factors were introduced for all nonhydrogen atoms. Further Fourier difference functions permitted location of nonmethyl hydrogen atoms, which were included in the refinement for three cycles of least squares and then held fixed; in the case of $[Fe^{III}(5\text{-}OCH_3Salmeen)_2]PF_6$ the methyl hydrogen atoms were also located from Fourier maps. The models converged with $R = 6.3\%$ and $R_w = 7.9\%$ for $[Fe^{III}(3\text{-}OCH_3Salmeen)_2]PF_6$, $R = 4.7\%$ and $R_w = 6.5\%$ for $[Fe^{III}(NO_2Salmeen)_2]PF_6$, and $R = 5.1\%$ and $R_w = 6.9\%$ for $[Fe^{III}(5\text{-}OCH_3Salmeen)_2]PF_6$. A structure factor calculation with all observed and unobserved reflections included (no refinement) gave

---

[30] Cromer, D. T.; Ibers, J. A. Reference 28.

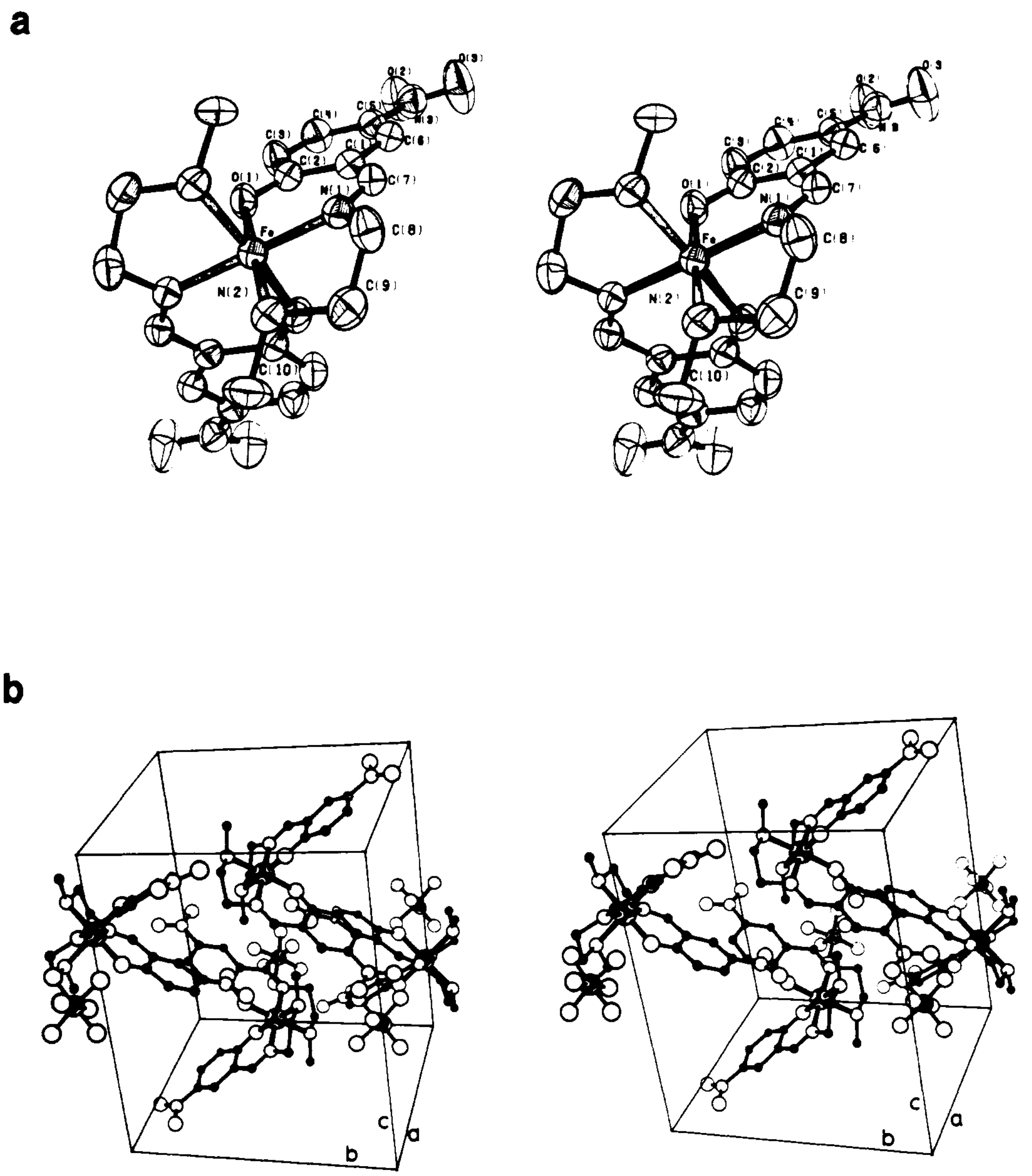

Figure 3. (a) Stereopair view of the [Fe^{III}(5-NO$_2$Salmeen)$_2$]$^+$ cation in [Fe^{III}(5-NO$_2$Salmeen)$_2$]PF$_6$. (b) Stereopair view of the molecular packing for the [Fe^{III}(5-NO$_2$Salmeen)$_2$]PF$_6$ salt.

R = 8.1, 5.4, and 5.8% for the three complexes respectively; on this basis it was decided that careful measurement of reflections rejected automatically during data collection would not significantly improve the results. A final Fourier difference function was featureless. Tables of the observed and calculated structure factors are available,[31] together with the hydrogen atomic parameters and the distances and angles within the PF$_6^-$ anions.[31] The principal programs used are as previously described.[32]

Results and Discussion

Final positional and thermal parameters for [Fe^{III}(3-OCH$_3$Salmeen)$_2$]PF$_6$, [Fe^{III}(NO$_2$Salmeen)$_2$]PF$_6$, and [Fe^{III}(5-OCH$_3$Salmeen)$_2$]PF$_6$ are given in Table I. Tables II and III contain the bond lengths and angles. The digits in parentheses in the tables are the estimated standard deviations in the least significant figures quoted and were derived from the inverse matrix in the course of least-squares refinement calculations. Figures 2–4 show stereoviews of the cations and the packing diagrams of the three complexes [Fe^{III}(3-OCH$_3$Salmeen)$_2$]PF$_6$, [Fe^{III}(5-NO$_2$Salmeen)$_2$]PF$_6$, and [Fe^{III}(5-OCH$_3$Salmeen)$_2$]PF$_6$, respectively.

[Fe^{III}(3-OCH$_3$Salmeen)$_2$]PF$_6$. The crystal structure of this complex consists of well-defined [Fe^{III}(3-OCH$_3$Salmeen)$_2$]$^+$ ions (Figure 2a) and disordered PF$_6^-$ ions. The complex cations are separated from one another by the PF$_6^-$ anions (Table II, Figure 2b), the closest interionic approaches being 2.94 Å [F(4′)–N(2A)] and 3.069 Å [F(6)–C(8B)]. The disorder in the PF$_6^-$ ions is essentially axial, consisting of two positions separated by a rotation of 45° about the F(1)–P–F(2) axis. The disorder is not entirely accounted for by these positions, but the remaining positions contribute significantly less electron density than the hydrogen atoms in the molecules. Since the complex cation is well-defined and the PF$_6^-$ ion was not of primary interest, this disorder problem was not pursued further. The metal environment in the complex cation is approximately octahedral, with the oxygen atoms of the two different ligands being cis to each other and the imino nitrogens of the two ligands being trans. The deviation from octahedral symmetry of the FeN$_4$O$_2$ unit is indicated by the bond lengths, angles, and interplanar angles. The angles O(1A)–Fe–N(2A), O(1B)–Fe–N(2B), and N(1A)–Fe–N(1B) all deviate some-

---

(31) Supplementary material.

(32) Freyberg, D. P.; Mockler, G. M.; Sinn, E. *J. Chem. Soc., Dalton Trans.* **1976**, 447.

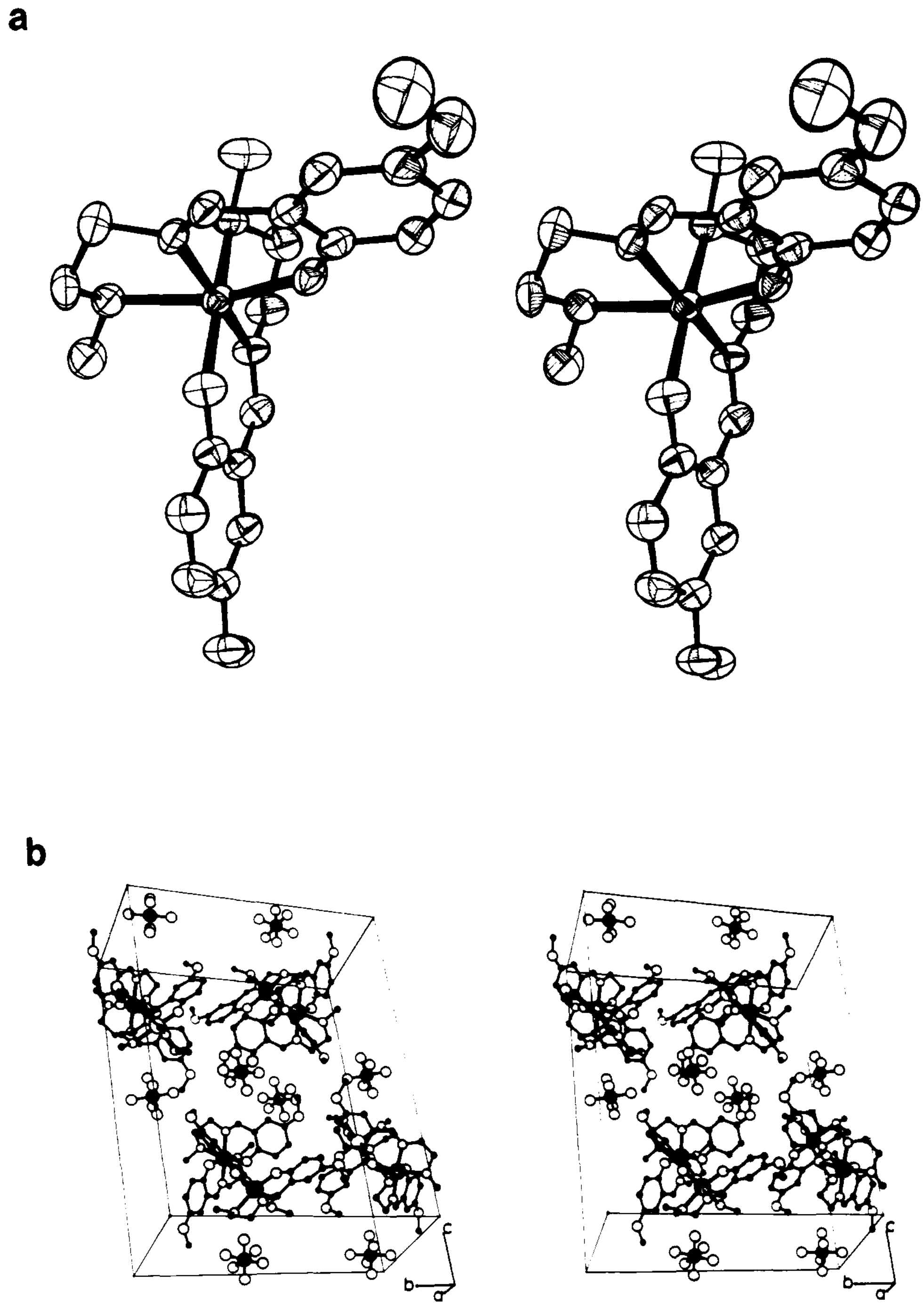

Figure 4. (a) Stereopair view of the [Fe^{III}(5-OCH$_3$Salmeen)$_2$]$^+$ cation in [Fe^{III}(5-OCH$_3$Salmeen)$_2$]PF$_6$. Atom labels are analogous to those of Figures 2a and 3a. (b) Stereopair view of the molecular packing for the [Fe^{III}(5-OCH$_3$Salmeen)$_2$]PF$_6$ salt.

what from the ideal octahedral 180° (175.0, 175.2, and 178.9°, respectively). In this regard the complex closely resembles (and is very slightly less distorted than) the $S = {}^1/_2$ low-spin hexadentate [Fe^{III}(Sal)$_2$trien]$^+$ cation (Figure 1b)[9,20] and is markedly less distorted than the high-spin hexadentate complexes [Fe^{III}(Acac)$_2$trien]$^+$ and [Fe^{III}(AcacCl)$_2$trien]$^+$ of Figure 1c.[9,21] The metal-ligand bond lengths are uneven: the two Fe–O bonds are by far the shortest (1.878 Å average), and the bonds to the amino nitrogen atoms are longer (2.060 Å) than those to the imino nitrogens (1.934 Å). In terms of these bond lengths, the cation is similar to (and very slightly more distorted than) the cations in the low-spin hexadentate complexes but much closer to octahedral geometry than those of the high-spin hexadentates. The 12 angles subtended at the metal atom by adjacent donor atoms range from 83.3 to 96.2°, compared to the 90° required for a perfect octahedron.

[Fe^{III}(5-NO$_2$Salmeen)$_2$]PF$_6$ ($S = {}^1/_2$). The crystal structure of this low-spin complex consists of well-defined [Fe^{III}(5-NO$_2$Salmeen)$_2$]$^+$ ions (Figure 3a) and disordered PF$_6^-$ ions, though, unlike the case of [Fe^{III}(3-OCH$_3$Salmeen)$_2$]PF$_6$, the PF$_6^-$ disorder is not by rotation about an F–P–F axis. The complex cations are separated from one another by disordered PF$_6^-$ anions (Table II, Figure 3b), the closest interionic separation being 3.036 Å [F(2′)–C(8)] and 3.042 Å [F(1)–N(2)]. In the 3-OCH$_3$ and 5-OCH$_3$ complexes (see below), the two ligands in the cation are related to one another by a pseudotwofold axis, but in [Fe^{III}(5-NO$_2$Salmeen)$_2$]$^+$ a precise twofold axis relates the ligands. The ligand environment in the complex cation is approximately octahedral, with the oxygen atoms of the two different ligands being cis to each other and the imino nitrogens trans. Again the angles O(1)–Fe–N(2), N(1)–Fe–N(1′), and O(1′)–Fe–N(2) deviate somewhat

Table I. Positional and Thermal Parameters and Their Estimated Standard Deviations[a]

atom	x	y	z	U_{11}	U_{22}	U_{33}	U_{12}	U_{13}	U_{23}
(a) $[Fe(3\text{-}OCH_3Salmeen)_2]PF_6$									
Fe	0.20297 (8)	0.1613 (1)	−0.09307 (5)	0.0264 (5)	0.0272 (6)	0.0241 (5)	0.0006 (5)	0.0007 (4)	0.0007 (5)
P	0.7012 (2)	0.2969 (3)	0.7521 (1)	0.050 (1)	0.070 (2)	0.045 (1)	−0.001 (1)	0.009 (1)	0.021 (1)
F(1)	0.7062 (6)	0.3001 (8)	0.6785 (3)	0.122 (5)	0.162 (7)	0.052 (3)	−0.014 (5)	0.033 (3)	0.024 (4)
F(2)	0.6929 (7)	0.2962 (8)	0.8234 (3)	0.163 (6)	0.137 (6)	0.044 (3)	−0.029 (5)	0.001 (4)	0.008 (4)
F(3)	0.6909 (11)	0.4516 (10)	0.7503 (4)	0.202 (11)	0.062 (6)	0.089 (6)	0.011 (7)	0.054 (6)	0.008 (6)
F(4)	0.8319 (8)	0.3139 (14)	0.7509 (7)	0.052 (6)	0.201 (13)	0.223 (13)	0.038 (7)	−0.004 (7)	0.064 (11)
F(5)	0.7166 (14)	0.1531 (10)	0.7490 (5)	0.295 (16)	0.058 (7)	0.102 (8)	−0.041 (9)	0.043 (9)	−0.005 (6)
F(6)	0.5728 (8)	0.2909 (15)	0.7488 (5)	0.047 (5)	0.270 (15)	0.097 (7)	−0.044 (7)	0.010 (5)	0.022 (9)
F(3′)	0.5975 (14)	0.1866 (19)	0.7418 (7)	0.091 (10)	0.151 (15)	0.044 (8)	−0.077 (10)	−0.013 (8)	0.021 (10)
F(4′)	0.8061 (16)	0.3843 (18)	0.7610 (8)	0.170 (12)	0.145 (12)	0.065 (10)	−0.143 (8)	−0.025 (9)	0.056 (9)
F(5′)	0.6128 (22)	0.1014 (21)	0.2410 (13)	0.175 (19)	0.097 (14)	0.191 (22)	−0.072 (13)	0.004 (17)	−0.070 (15)
F(6′)	0.7744 (16)	0.3271 (19)	0.2632 (9)	0.084 (11)	0.087 (13)	0.111 (14)	−0.031 (10)	−0.018 (11)	−0.046 (11)
O(1A)	0.2846 (4)	0.2386 (5)	−0.0259 (2)	0.043 (3)	0.030 (3)	0.027 (3)	−0.010 (3)	−0.002 (2)	−0.002 (2)
O(2A)	0.4149 (5)	0.3765 (5)	0.0494 (2)	0.056 (3)	0.038 (3)	0.048 (3)	−0.018 (3)	−0.011 (3)	0.001 (3)
O(1B)	0.0606 (4)	0.2351 (5)	−0.0760 (2)	0.033 (3)	0.018 (3)	0.040 (3)	0.004 (2)	0.006 (2)	0.002 (2)
O(2B)	−0.1384 (4)	0.3033 (5)	−0.0344 (3)	0.042 (3)	0.033 (3)	0.063 (3)	0.008 (3)	0.015 (3)	0.008 (3)
N(1A)	0.1591 (5)	0.0143 (6)	−0.0449 (3)	0.029 (3)	0.020 (3)	0.036 (3)	0.001 (3)	0.006 (3)	−0.004 (3)
N(2A)	0.1215 (5)	0.0624 (6)	−0.1645 (3)	0.040 (3)	0.041 (4)	0.027 (3)	−0.001 (3)	−0.005 (3)	−0.002 (3)
N(1B)	0.2489 (5)	0.3064 (6)	−0.1421 (3)	0.042 (3)	0.027 (4)	0.029 (3)	−0.003 (3)	0.001 (3)	0.003 (3)
N(2B)	0.3573 (5)	0.0848 (6)	−0.1194 (3)	0.025 (3)	0.039 (4)	0.036 (3)	0.002 (3)	0.006 (3)	−0.002 (3)
C(1A)	0.2430 (6)	0.0829 (7)	0.0536 (3)	0.032 (4)	0.031 (4)	0.027 (4)	0.008 (4)	0.004 (3)	0.001 (4)
C(2A)	0.2931 (6)	0.1981 (7)	0.0318 (3)	0.031 (4)	0.030 (4)	0.026 (4)	0.003 (4)	−0.002 (3)	0.002 (4)
C(3A)	0.3643 (6)	0.2717 (8)	0.0738 (4)	0.038 (4)	0.032 (5)	0.041 (4)	0.006 (4)	−0.003 (4)	−0.002 (4)
C(4A)	0.3776 (7)	0.2353 (9)	0.1357 (4)	0.050 (5)	0.050 (6)	0.037 (4)	−0.002 (5)	−0.004 (4)	−0.008 (4)
C(5A)	0.3270 (7)	0.1208 (9)	0.1554 (3)	0.055 (5)	0.062 (6)	0.025 (4)	0.005 (5)	0.001 (4)	0.003 (4)
C(6A)	0.2612 (7)	0.0474 (8)	0.1165 (3)	0.038 (4)	0.050 (5)	0.030 (4)	0.005 (4)	0.007 (3)	0.011 (4)
C(7A)	0.1763 (6)	−0.0007 (7)	0.0148 (3)	0.036 (4)	0.025 (4)	0.036 (4)	0.001 (4)	0.011 (3)	0.004 (4)
C(8A)	0.0970 (7)	−0.0857 (8)	−0.0808 (4)	0.047 (5)	0.031 (5)	0.045 (5)	−0.008 (4)	0.005 (4)	−0.008 (4)
C(9A)	0.0361 (7)	−0.0192 (9)	−0.1353 (4)	0.038 (4)	0.051 (6)	0.050 (5)	−0.011 (4)	−0.005 (4)	−0.015 (5)
C(10A)	0.0635 (8)	0.1420 (10)	−0.2145 (4)	0.066 (5)	0.076 (7)	0.045 (5)	0.012 (6)	−0.030 (4)	−0.001 (5)
C(11A)	0.4954 (9)	0.4509 (10)	0.0883 (5)	0.077 (6)	0.064 (7)	0.072 (6)	−0.031 (5)	−0.031 (5)	−0.006 (6)
C(1B)	0.0949 (6)	0.4492 (8)	−0.1169 (3)	0.039 (4)	0.031 (5)	0.035 (4)	−0.003 (4)	−0.003 (4)	0.003 (4)
C(2B)	0.0315 (6)	0.3572 (7)	−0.0852 (3)	0.039 (4)	0.028 (4)	0.029 (4)	0.003 (4)	−0.005 (3)	−0.002 (4)
C(3B)	−0.0790 (7)	0.3979 (8)	−0.0627 (3)	0.048 (5)	0.033 (5)	0.032 (4)	0.009 (4)	−0.002 (4)	0.001 (4)
C(4B)	−0.1157 (7)	0.5218 (8)	−0.0711 (4)	0.046 (5)	0.031 (5)	0.065 (6)	0.010 (4)	0.003 (4)	−0.001 (5)
C(5B)	−0.0520 (8)	0.6095 (8)	−0.1016 (5)	0.065 (6)	0.023 (5)	0.082 (6)	0.011 (5)	−0.009 (5)	−0.003 (5)
C(6B)	0.0501 (8)	0.5756 (8)	−0.1246 (4)	0.060 (5)	0.033 (5)	0.060 (5)	−0.016 (4)	−0.002 (5)	0.004 (5)
C(7B)	0.2012 (7)	0.4168 (8)	−0.1447 (3)	0.054 (5)	0.034 (5)	0.028 (4)	−0.012 (4)	−0.003 (4)	0.007 (4)
C(8B)	0.3566 (7)	0.2846 (9)	−0.1749 (4)	0.043 (4)	0.057 (6)	0.041 (4)	0.002 (5)	0.017 (4)	0.010 (5)
C(9B)	0.4291 (7)	0.1970 (9)	0.1347 (4)	0.036 (4)	0.060 (6)	0.052 (5)	0.003 (4)	0.009 (4)	0.019 (5)
C(10B)	0.4204 (7)	−0.0008 (9)	−0.0722 (4)	0.040 (4)	0.052 (6)	0.056 (5)	0.025 (4)	−0.001 (4)	0.006 (5)
C(11B)	−0.2517 (7)	0.3353 (10)	−0.0156 (5)	0.042 (5)	0.065 (7)	0.093 (7)	0.015 (5)	0.027 (5)	0.009 (6)
(b) $[Fe(NO_2Salmeen)_2]PF_6$									
Fe	0.0000 (0)	0.01283 (5)	0.2500 (0)	0.0332 (3)	0.0491 (4)	0.0354 (3)	0.0000 (0)	0.0010 (2)	0.0000 (0)
P	0.5000 (0)	0.1121 (1)	0.2500 (0)	0.0543 (9)	0.0560 (9)	0.149 (2)	0.0000 (0)	0.0174 (9)	0.0000 (0)
F(1)	0.4504 (4)	0.1941 (3)	0.3094 (3)	0.216 (4)	0.105 (3)	0.220 (4)	−0.028 (3)	0.137 (3)	−0.041 (3)
F(2)	0.4519 (3)	0.0357 (3)	0.3143 (3)	0.098 (2)	0.109 (2)	0.185 (4)	−0.005 (2)	0.002 (3)	0.065 (3)
F(3)	0.4013 (4)	0.1278 (6)	0.1979 (5)	0.101 (3)	0.298 (7)	0.263 (6)	0.070 (3)	−0.063 (4)	−0.003 (6)
F(1′)	0.4318 (8)	0.2049 (6)	0.2801 (6)	0.104 (7)	0.050 (4)	0.117 (7)	0.035 (4)	0.024 (6)	0.033 (5)
F(2′)	0.4188 (9)	0.0330 (10)	0.2640 (13)	0.077 (6)	0.104 (7)	0.483 (22)	−0.048 (6)	0.116 (9)	−0.130 (9)
F(3′)	0.4118 (13)	0.0643 (15)	0.1976 (9)	0.236 (14)	0.243 (14)	0.090 (8)	−0.119 (11)	−0.021 (11)	−0.009 (10)
O(1)	0.0463 (2)	0.1150 (2)	0.1748 (1)	0.034 (1)	0.061 (1)	0.052 (1)	0.000 (1)	0.002 (1)	0.011 (1)
O(2)	−0.1567 (3)	0.4889 (2)	−0.0090 (2)	0.078 (2)	0.073 (2)	0.118 (3)	0.001 (1)	−0.008 (2)	0.039 (1)
O(3)	−0.2898 (2)	0.3875 (3)	−0.0060 (2)	0.059 (2)	0.114 (2)	0.147 (3)	0.006 (2)	−0.015 (2)	0.061 (2)
N(1)	−0.1423 (2)	0.0100 (2)	0.2035 (2)	0.038 (1)	0.049 (1)	0.043 (1)	−0.004 (1)	0.003 (1)	−0.003 (1)
N(2)	−0.0604 (2)	−0.0978 (2)	0.3276 (2)	0.045 (1)	0.059 (2)	0.037 (1)	−0.003 (1)	0.005 (1)	0.001 (1)
N(3)	−0.1968 (2)	0.4060 (3)	0.0082 (2)	0.052 (2)	0.075 (2)	0.066 (2)	0.008 (2)	0.003 (1)	0.013 (2)
C(1)	−0.1265 (2)	0.1683 (2)	0.1263 (2)	0.040 (2)	0.052 (2)	0.038 (2)	0.002 (1)	0.003 (1)	−0.003 (1)
C(2)	−0.0146 (2)	0.1814 (2)	0.1372 (2)	0.041 (2)	0.050 (2)	0.044 (2)	0.001 (1)	0.004 (1)	−0.002 (1)
C(3)	0.0323 (3)	0.2697 (3)	0.1019 (2)	0.043 (2)	0.062 (2)	0.069 (2)	−0.005 (2)	−0.002 (2)	0.010 (2)
C(4)	−0.0257 (3)	0.3427 (3)	0.0612 (2)	0.057 (2)	0.055 (2)	0.064 (2)	−0.007 (2)	−0.001 (2)	0.012 (2)
C(5)	−0.1349 (3)	0.3281 (3)	0.0508 (2)	0.047 (2)	0.055 (2)	0.046 (2)	0.011 (2)	0.002 (2)	0.006 (2)
C(6)	−0.1831 (2)	0.2421 (3)	0.0816 (2)	0.036 (2)	0.062 (2)	0.045 (2)	0.003 (2)	0.001 (1)	−0.004 (2)
C(7)	−0.1830 (2)	0.0798 (3)	0.1576 (2)	0.034 (1)	0.059 (2)	0.041 (2)	0.000 (2)	−0.001 (1)	−0.005 (2)
C(8)	−0.2065 (3)	−0.0784 (3)	0.2321 (2)	0.040 (2)	0.057 (2)	0.068 (2)	−0.011 (2)	−0.004 (2)	0.003 (2)
C(9)	−0.1777 (3)	−0.0937 (3)	0.3218 (2)	0.047 (2)	0.067 (2)	0.060 (2)	−0.009 (2)	0.012 (2)	0.006 (2)
C(10)	−0.0255 (3)	−0.0925 (3)	0.4166 (2)	0.077 (2)	0.098 (3)	0.036 (2)	−0.016 (2)	−0.006 (2)	0.011 (2)
(c) $[Fe(5\text{-}OCH_3Salmeen)_2]PF_6$									
Fe	0.08933 (7)	0.11042 (4)	0.15319 (3)	0.0309 (4)	0.0411 (4)	0.0350 (4)	−0.0003 (4)	0.0037 (4)	−0.0025 (4)
P	0.2219 (2)	0.11693 (9)	0.49092 (6)	0.048 (1)	0.068 (1)	0.0468 (9)	−0.0060 (9)	0.0058 (8)	−0.0088 (9)
F(1)	0.2222 (4)	0.1068 (2)	0.4312 (1)	0.086 (3)	0.116 (3)	0.047 (2)	−0.011 (3)	−0.000 (2)	−0.012 (2)
F(2)	0.2591 (4)	0.1936 (2)	0.4831 (2)	0.103 (3)	0.068 (2)	0.092 (3)	−0.009 (3)	0.009 (3)	0.001 (2)
F(3)	0.1875 (6)	0.0404 (2)	0.4978 (2)	0.205 (5)	0.072 (3)	0.083 (3)	−0.042 (3)	0.031 (3)	−0.010 (2)
F(4)	0.3740 (4)	0.0986 (3)	0.4903 (2)	0.057 (2)	0.154 (4)	0.082 (3)	0.033 (3)	0.008 (2)	0.011 (3)

Table I (*Continued*)

atom	x	y	z	U_{11}	U_{22}	U_{33}	U_{12}	U_{13}	U_{23}
F(5)	0.0734 (4)	0.1366 (3)	0.4900 (2)	0.044 (2)	0.191 (5)	0.092 (3)	0.003 (3)	0.005 (2)	−0.010 (3)
F(6)	0.2258 (4)	0.1265 (2)	0.5493 (1)	0.086 (3)	0.109 (3)	0.046 (2)	−0.011 (3)	0.007 (2)	−0.013 (2)
O(1A)	0.1571 (3)	0.1869 (2)	0.1888 (1)	0.033 (2)	0.054 (2)	0.043 (2)	−0.007 (2)	0.008 (2)	−0.008 (2)
O(2A)	0.0691 (4)	0.3051 (2)	0.3727 (2)	0.064 (3)	0.081 (3)	0.055 (2)	−0.017 (2)	0.015 (2)	−0.031 (2)
O(1B)	0.1976 (4)	0.0416 (2)	0.1820 (1)	0.048 (2)	0.060 (2)	0.038 (2)	0.009 (2)	0.005 (2)	0.008 (2)
O(2B)	0.6326 (4)	−0.1029 (2)	0.1251 (2)	0.044 (2)	0.062 (2)	0.065 (3)	0.019 (2)	0.002 (2)	0.011 (2)
N(1A)	−0.0602 (4)	0.1071 (2)	0.2062 (2)	0.028 (2)	0.042 (2)	0.047 (3)	−0.006 (2)	0.002 (2)	−0.006 (2)
N(2A)	−0.0384 (4)	0.0294 (2)	0.1223 (2)	0.041 (3)	0.043 (2)	0.042 (3)	−0.001 (2)	0.001 (2)	−0.007 (2)
N(1B)	0.2217 (4)	0.1137 (2)	0.0930 (2)	0.038 (3)	0.048 (2)	0.038 (2)	0.009 (2)	0.005 (2)	0.009 (2)
N(2B)	−0.0073 (4)	0.1806 (2)	0.1014 (2)	0.040 (3)	0.043 (3)	0.047 (3)	0.011 (2)	−0.003 (2)	−0.003 (2)
C(1A)	0.0276 (5)	0.1901 (3)	0.2640 (2)	0.028 (3)	0.044 (3)	0.046 (3)	0.003 (3)	−0.002 (3)	−0.005 (3)
C(2A)	0.1288 (5)	0.2144 (3)	0.2330 (2)	0.029 (3)	0.046 (3)	0.039 (3)	0.005 (3)	−0.003 (3)	−0.003 (3)
C(3A)	0.2013 (5)	0.2697 (3)	0.2500 (2)	0.037 (3)	0.043 (3)	0.050 (3)	−0.003 (3)	0.001 (3)	−0.003 (3)
C(4A)	0.1787 (5)	0.2988 (3)	0.2958 (2)	0.037 (3)	0.045 (3)	0.058 (4)	−0.002 (3)	−0.005 (3)	−0.009 (3)
C(5A)	0.0790 (5)	0.2732 (3)	0.3272 (2)	0.039 (3)	0.054 (3)	0.047 (3)	0.004 (3)	0.002 (3)	−0.016 (3)
C(6A)	0.0063 (5)	0.2201 (3)	0.3111 (2)	0.034 (3)	0.057 (3)	0.045 (3)	−0.002 (3)	0.002 (3)	−0.004 (3)
C(7A)	−0.0629 (5)	0.1384 (3)	0.2479 (2)	0.029 (3)	0.049 (3)	0.043 (3)	−0.004 (3)	0.004 (3)	−0.003 (3)
C(8A)	−0.1671 (6)	0.0592 (3)	0.1944 (2)	0.045 (4)	0.057 (4)	0.052 (4)	−0.015 (3)	0.003 (3)	−0.004 (3)
C(9A)	−0.1094 (6)	0.0013 (3)	0.1660 (2)	0.054 (4)	0.043 (3)	0.064 (4)	−0.020 (3)	0.005 (3)	−0.004 (3)
C(10A)	0.0261 (7)	−0.0229 (3)	0.0922 (3)	0.061 (4)	0.069 (4)	0.076 (4)	−0.004 (4)	0.005 (4)	−0.032 (4)
C(11A)	−0.0202 (8)	0.2786 (4)	0.4070 (3)	0.087 (5)	0.110 (5)	0.063 (4)	−0.018 (5)	0.021 (4)	−0.038 (4)
C(1B)	0.3691 (5)	0.0262 (3)	0.1225 (2)	0.031 (3)	0.042 (3)	0.041 (3)	−0.001 (3)	−0.001 (3)	0.004 (3)
C(2B)	0.3019 (5)	0.0089 (3)	0.1664 (2)	0.036 (3)	0.047 (3)	0.039 (3)	0.003 (3)	−0.003 (3)	−0.002 (3)
C(3B)	0.3480 (6)	−0.0470 (3)	0.1945 (2)	0.054 (4)	0.056 (4)	0.047 (3)	0.002 (3)	0.009 (3)	0.014 (3)
C(4B)	0.4595 (6)	−0.0819 (3)	0.1797 (2)	0.060 (4)	0.052 (3)	0.054 (4)	0.011 (3)	−0.005 (3)	0.015 (3)
C(5B)	0.5253 (6)	−0.0638 (3)	0.1362 (2)	0.035 (3)	0.047 (3)	0.061 (4)	0.000 (3)	−0.007 (3)	0.003 (3)
C(6B)	0.4823 (5)	−0.0105 (3)	0.1082 (2)	0.036 (3)	0.054 (3)	0.044 (3)	0.002 (3)	0.001 (3)	0.005 (3)
C(7B)	0.3255 (5)	0.0784 (3)	0.0890 (2)	0.039 (3)	0.054 (3)	0.039 (3)	−0.002 (3)	0.008 (3)	0.005 (3)
C(8B)	0.1884 (6)	0.1610 (3)	0.0523 (2)	0.053 (4)	0.062 (4)	0.051 (4)	0.013 (3)	0.010 (3)	0.022 (3)
C(9B)	0.0966 (6)	0.2149 (3)	0.0736 (2)	0.065 (4)	0.050 (3)	0.059 (4)	0.002 (4)	0.002 (4)	0.018 (3)
C(10B)	−0.0939 (7)	0.2300 (4)	0.1258 (3)	0.068 (4)	0.079 (4)	0.067 (4)	0.033 (4)	0.000 (4)	−0.005 (4)
C(11B)	0.6805 (6)	−0.0996 (3)	0.0752 (3)	0.043 (3)	0.066 (4)	0.080 (5)	0.014 (3)	0.001 (4)	−0.000 (4)

[a] The form of the anisotropic thermal parameter is $\exp[-2\pi^2(U_{11}h^2a^{*2} + U_{22}k^2b^{*2} + U_{33}l^2c^{*2} + 2U_{12}hka^*b^* + 2U_{13}hla^*c^* + 2U_{23}klb^*c^*)]$.

from the ideal octahedral 180° (176.0, 179.9, and 176.0°, respectively). In this regard, the complex closely resembles the low-spin $[Fe^{III}(Sal)_2trien]^+$ (Figure 1b) and $[Fe^{III}(3\text{-}OCH_3Salmeen)_2]^+$ cations and is markedly less distorted than the high-spin hexadentate $[Fe^{III}(Acac)_2trien]^+$ and $[Fe^{III}(AcacCl)_2trien]^+$ complexes (Figures 1c). The metal–ligand bonds are again uneven: the two Fe–O bonds are by far the shortest (1.886 Å), and the bonds to the amino nitrogens are longer (2.046 Å) than those to the imino nitrogens (1.944 Å). However, the differences in these bond lengths are slightly smaller than in the analogous $[Fe^{III}(3\text{-}OCH_3Salmeen)_2]PF_6$ compound and therefore correspond to a slightly closer approach to octahedral symmetry. The 12 angles subtended at the metal atom by the adjacent donor atoms range from 83.0 to 95.5°, compared to the 90° required for a perfect octahedron.

$[Fe^{III}(5\text{-}OCH_3Salmeen)_2PF_6$ ($S = {}^5/_2$). The lattice of this high-spin complex consists of well-defined $[Fe^{III}(5\text{-}OCH_3Salmeen)_2]^+$ ions (Figure 3a) and PF_6^- anions; the latter in this case are not disordered. The metal environment in the complex cation is approximately octahedral and is qualitatively similar to that observed in the two low-spin Salmeen complexes described above, but with the distortions from octahedral symmetry being much greater than in either of these two complexes. The angles O(1A)–Fe–N(2A), O(1B)–Fe–N(2B), and N(1A)–Fe–N(1B) all deviate considerably from the ideal octahedral 180° (164.6, 164.2, and 172.9°, respectively). In this regard the complex differs dramatically from the low-spin Salmeen complexes but is similar to, though very slightly less distorted than, the high-spin hexadentate complexes $[Fe^{III}(Acac)_2trien]PF_6$ and $[Fe^{III}(AcacCl)_2trien]PF_6$. To an even greater extent than in its low-spin analogues, the metal–ligand bond lengths in $[Fe^{III}(5\text{-}OCH_3Salmeen)_2]^+$ are asymmetric, the Fe–O bonds being the shortest (1.914 Å average), and the bonds to the amino nitrogens are much longer (2.209 Å) than those to the imino nitrogens (2.100 Å). The bond asymmetry is similar to but slightly greater than that observed in the high-spin $[Fe^{III}(Acac)_2trien]^+$ and $[Fe^{III}(AcacCl)_2trien]^+$ complexes. The 12 angles subtended at the metal atom by adjacent donors range from 77.8 to 98.4°, compared with the 90° required for a perfect octahedron. This compares with the slightly larger ranges of 76.6–102.1° and 78.2–99.7° observed for $[Fe^{III}(Acac)_2trien]^+$ and $[Fe^{III}(AcacCl)_2trien]^+$, respectively.

Spin State/Structure Correlation for the $[Fe^{III}(X\text{-}Salmeen)_2]^+$ Complexes. As previously reported,[26] the $[Fe^{III}(X\text{-}Salmeen)_2]PF_6$ series of complexes displays a temperature-dependent $(S = {}^1/_2) \rightleftarrows (S = {}^5/_2)$ spin equilibrium in both the solid and solution states. In the solid state, at room temperature, the position of the spin equilibrium is X-substituent dependent (Figure 1a) with the X = H, 4-OCH_3, and 5-OCH_3 derivatives being $S = {}^5/_2$ species ($\mu_{eff}{}^{RT} > 5.7\ \mu_B$), whereas the 3-$OCH_3$ ($\mu_{eff}{}^{298} = 3.20\ \mu_B$) and 5-$NO_2$ ($\mu_{eff}{}^{295} = 2.58\ \mu_B$) derivatives are more nearly $S = {}^1/_2$ compounds. With assumption of limiting magnetic moments of 5.9 and 2.0 μ_B for the fully $S = {}^5/_2$ and $S = {}^1/_2$ states,[26] the 5-OCH_3 compound can therefore be considered to be 95% high spin, while the 3-OCH_3 and 5-NO_2 derivatives are 70% and 92% low spin, respectively. Thus, a comparison of molecular structures for the three $[Fe^{III}(XSalmeen)_2]^+$ cations with X = 5-OCH_3, 3-OCH_3, and 5-NO_2 reflects the spin state dependent structural changes associated with a ≥90% $(S = {}^5/_2) \rightarrow (S = {}^1/_2)$ spin conversion. In the present work, no attempt has been made to crystallographically resolve structures for the two $S = {}^1/_2$ and $S = {}^5/_2$ spin isomers in the same crystal lattice; i.e., only the "average" structure is reported, although in theory the 3-OCH_3 compound (70% low spin) might lend itself well to such an attempt.[10]

As noted above, the high-spin 5-OCH_3 complex has an N_4O_2 coordination sphere that is much more distorted from an oc-

Table II

Bond Distances (A) for [$Fe^{III}(3\text{-}OCH_3Salmeen)_2]PF_6$, [$Fe^{III}(5\text{-}NO_2Salmeen)_2]PF_6$, and [$Fe^{III}(5\text{-}OCH_3Salmeen)_2]PF_6$

atoms	3-OCH_3	NO_2	5-OCH_3	atoms	3-OCH_3	NO_2	5-OCH_3
Fe–O(1A)	1.880 (2)	1.886 (1)	1.913 (2)	N(2A)–C(10A)	1.498 (5)	1.485 (2)	1.466 (4)
Fe–O(1B)	1.877 (2)		1.915 (2)	N(2B)–C(10B)	1.519 (5)		1.472 (4)
Fe–N(1A)	1.933 (3)	1.944 (1)	2.092 (3)	N(3)–C(5)		1.448 (2)	
Fe–N(1B)	1.934 (3)		2.108 (3)	C(1A)–C(2A)	1.423 (5)	1.430 (2)	1.413 (4)
Fe–N(2A)	2.053 (3)	2.046 (1)	2.224 (3)	C(1B)–C(2B)	1.405 (5)		1.404 (4)
Fe–N(2B)	2.067 (3)		2.194 (3)	C(1A)–C(6A)	1.415 (5)	1.393 (2)	1.409 (4)
O(1A)–C(2A)	1.317 (4)	1.302 (2)	1.334 (4)	C(1B)–C(6B)	1.423 (6)		1.421 (4)
O(1B)–C(2B)	1.328 (4)		1.317 (4)	C(1A)–C(7A)	1.416 (5)	1.439 (2)	1.443 (4)
O(2A)–C(3A)	1.358 (5)			C(1B)–C(7B)	1.439 (6)		1.435 (4)
O(2A)–C(5A)			1.375 (4)	C(2A)–C(3A)	1.425 (5)	1.408 (2)	1.395 (4)
O(2A)–C(11A)	1.453 (5)		1.398 (5)	C(2B)–C(3B)	1.458 (6)		1.415 (4)
O(2B)–C(3B)	1.364 (5)			C(3A)–C(4A)	1.393 (6)	1.364 (3)	1.375 (5)
O(2B)–C(5B)			1.376 (4)	C(3B)–C(4B)	1.368 (6)		1.392 (5)
O(2B)–C(11B)	1.436 (5)		1.426 (1)	C(4A)–C(5A)	1.404 (6)	1.400 (2)	1.416 (5)
O(2)–N(3)		1.216 (2)		C(4B)–C(5B)	1.364 (6)		1.392 (5)
O(3)–N(3)		1.217 (2)		C(5A)–C(6A)	1.349 (6)	1.363 (2)	1.356 (4)
N(1A)–C(7A)	1.307 (5)	1.276 (2)	1.275 (4)	C(5B)–C(6B)	1.355 (6)		1.363 (4)
N(1B)–C(7B)	1.277 (5)		1.277 (4)	C(8A)–C(9A)	1.515 (6)	1.503 (3)	1.494 (5)
N(1A)–C(8A)	1.468 (5)	1.476 (2)	1.481 (4)	C(8B)–C(9B)	1.495 (6)		1.528 (5)
N(1B)–C(8B)	1.485 (5)		1.473 (4)	⟨C–H⟩		0.95	0.94
N(2A)–C(9A)	1.471 (5)	1.481 (2)	1.484 (4)				
N(2B)–C(9B)	1.482 (5)		1.466 (4)				

Interionic Contacts (Å)

		(a) [$Fe^{III}(3\text{-}OCH_3Salmeen)_2]PF_6$			
O(2B)	C(7A)	3.212 (5)^a	F(6)	C(8B)	3.069 (8)^c
F(3)	N(2A)	3.15 (1)^b	F(6)	C(9B)	3.24 (1)^c
F(3)	N(2B)	3.180 (9)^b	F(4′)	N(2A)	2.94 (2)^b
F(4)	N(2A)	3.25 (1)^b			
		(b) [$Fe^{III}(5\text{-}NO_2Salmeen)_2]PF_6$			
F(1)	N(2)	3.042 (6)^d	F(2′)	C(8)	3.04 (3)^f
F(1′)	N(2)	3.09 (3)^e			
		(c) [$Fe^{III}(5\text{-}OCH_3Salmeen)_2]PF_6$			
F(1)	N(2A)	3.228 (4)^g	F(4)	N(2B)	3.183 (4)^g
F(1)	N(2B)	3.254 (4)^g	O(2B)	C(10B)	3.314^h

[a] $-x, -y, -z$. [b] $1 - x, {}^1/_2 + y, {}^1/_2 - z$. [c] $x, y, 1 + z$. [d] ${}^1/_2 - x, {}^1/_2 + y, z$. [e] ${}^1/_2 + x, {}^1/_2 + y, {}^1/_2 - z$. [f] $-x, y, {}^1/_2 - z$. [g] ${}^1/_2 + x, y, {}^1/_2 - z$. [h] ${}^1/_2 - x, y - {}^1/_2, z$.

tahedral arrangement of donor atoms than for either of the low-spin 3-OCH_3 or 5-NO_2 derivatives. This fact is evidenced by comparing the range of internal N–Fe–N and N–Fe–O bond angles which span from 78.3 to 96.7° for 5-OCH_3, as compared to only 83.3–95.6° and 83.0–95.5° for 3-OCH_3 and 5-NO_2, respectively (90° is required for a perfect octahedron), and the range of the six Fe–ligand bond distances which vary from 1.91 to 2.21 Å (Δ = 0.30 Å) in 5-OCH_3 and only from 1.88 to 2.04 Å (Δ = 0.16 Å) in the two low-spin complexes. Table IV summarizes the average Fe–ligand bond distances for the three complexes. Inspection of the table reveals that the deviation from octahedralicity for all three [Fe^{III}(X-Salmeen)$_2]^+$ cations is characterized by markedly uneven Fe–ligand bond lengths: the two Fe–O bonds are by far the shortest (the phenolic oxygens bear negative charge), and the bonds to the amino nitrogen atoms are longer than those to the imino nitrogens. Furthermore, this distortion pattern is common to both the high-spin and low-spin forms, although it is more accentuated in the high-spin 5-OCH_3 complexes where all the Fe–ligand bond distances are longer due to double occupancy of the e_g* (under O_h symmetry) orbitals.

The average Fe–ligand distance in the high-spin 5-OCH_3 complex, r_{hs}, is 2.074 Å, whereas in the low-spin 5-NO_2 complex the distance r_{ls} is 1.959 Å. This gives an average difference, δ_{av}, between the high-spin and low-spin forms of approximately 0.12 Å. Using the corresponding r_{ls} = 1.957 Å data from the 3-OCH structure gives the same result for δ_{av}, even though magnetic data (vide supra) suggest that the compound is only 70% low spin. It is instructive to compare this δ_{av} = 0.12 Å result for the present $3d^5$ (and $3d^6$) spin-equilibrium systems; this information has been collected in Table V. The complexes in the table are all six-coordinate species derived from different ligands having various dentate character and donor atom sets. For comparison with the present bis tridentate [Fe^{III}(X-Salmeen)$_2]^+$ series, the structurally similar hexadentate [Fe^{III}(Sal)$_2$trien]$^+$ and [Fe^{III}(Acac)$_2$trien]$^+$ complexes of Figure 1b,c are probably the most relevant[9] in that both the bis tridentate and hexadentate complexes have the same N_4O_2 donor atom set arranged in the same manner about the metal atom. The two series of complexes are further related in that they exhibit the same tetragonal distortion pattern in both spin isomers, although it is much less pronounced in the low-spin forms. For example, the high-spin [Fe^{III}(Acac)$_2$trien]PF_6 complex (Figure 1c with X = H) has Fe–N(amino) = 2.17 Å, Fe–N(imino) = 2.10 Å, and Fe–O = 1.93 Å, which compares to corresponding distances of 2.21, 2.10, and 1.91 Å in the high-spin [Fe^{III}(5-OCH_3Salmeen)$_2]PF_6$ compound. For the low-spin [Fe^{III}(Sal)$_2$trien]$NO_3 \cdot H_2O$ complex (Figure 1b), Fe–N(amino) = 2.00 Å, Fe–N(imino) = 1.93 Å, and Fe–O = 1.88 Å, whereas the corresponding distances in the low-spin [Fe^{III}(5-NO_2Salmeen)$_2]PF_6$ complex are 2.05, 1.94, and 1.89 Å, respectively. These spin state dependent bond distance changes result in the same δ_{av} = 0.12–0.13 Å value for both the hexadentates and present bis tridentates, except that in the [Fe^{III}(XSalmeen)$_2]^+$ complexes the Fe–N(amino) bond is considerably longer (0.04–0.05 Å) for both spin states than the corresponding distance in the hexadentate species (by comparison, the Fe–N(imino) and Fe–O distances differ by only 0.01–0.02 Å). Of course, the constraining influence of

Table III. Bond Angles (Deg) for $[Fe^{III}(3\text{-}OCH_3Salmeen)_2]PF_6$, $[Fe^{III}(5\text{-}NO_2Salmeen)_2]PF_6$, and $[Fe^{III}(5\text{-}OCH_3Salmeen)_2]PF_6$

atoms	$3\text{-}OCH_3$	NO_2	$5\text{-}OCH_3$
O(1A)–Fe–O(1B)	95.3 (1)	91.1 (1)	98.4 (1)
O(1A)–Fe–N(1A)	93.4 (1)	92.9 (1)	87.3 (1)
O(1A)–Fe–N(2A)	175.0 (1)	176.0 (1)	164.6 (1)
O(1A)–Fe–N(1B)	87.0 (1)	88.6 (1)	97.0 (1)
O(1A)–Fe–N(2B)	87.9 (1)	88.9 (1)	89.0 (1)
O(1B)–Fe–N(1A)	87.8 (1)		97.5 (1)
O(1B)–Fe–N(2A)	88.4 (1)		89.0 (1)
O(1B)–Fe–N(1B)	93.2 (1)		87.4 (1)
O(1B)–Fe–N(2B)	175.2 (1)		164.2 (1)
N(1A)–Fe–N(2A)	83.3 (1)	83.0 (1)	78.3 (1)
N(1A)–Fe–N(1B)	178.9 (1)	177.9 (1)	172.9 (1)
N(1A)–Fe–N(2B)	95.6 (1)	95.5 (1)	96.7 (1)
N(2A)–Fe–N(1B)	96.2 (1)		96.8 (1)
N(2A)–Fe–N(2B)	88.6 (1)	91.4 (1)	87.2 (1)
N(1B)–Fe–N(2B)	83.4 (1)		77.8 (1)
Fe–O(1A)–C(2A)	127.5 (2)	125.3 (1)	133.0 (2)
Fe–O(1B)–C(2B)	125.7 (2)		133.6 (2)
C(3A)–O(2A)–C(11A)	118.9 (3)		
C(5A)–O(2A)–C(11A)			117.4 (3)
C(3B)–O(2B)–C(11B)	116.7 (3)		
C(5B)–O(2B)–C(11B)			116.9 (2)
Fe–N(1A)–C(7A)	126.5 (3)	125.7 (1)	126.5 (2)
Fe–N(1B)–C(7B)	126.7 (3)		125.8 (2)
Fe–N(1A)–C(8A)	114.4 (2)		114.7 (2)
C(2A)–C(3A)–C(4A)	120.1 (4)	121.9 (2)	121.8 (3)
C(2B)–C(3B)–C(4B)	120.3 (4)		120.5 (3)
O(2A)–C(3A)–C(2A)	115.8 (3)		
O(2A)–C(3A)–C(4A)	124.1 (4)		
O(2B)–C(3B)–C(2B)	114.3 (3)		
O(2B)–C(3B)–C(4B)	125.4 (4)		
C(3A)–C(4A)–C(5A)	119.6 (4)	119.6 (2)	120.1 (3)
C(3B)–C(4B)–C(5B)	121.5 (4)		120.7 (3)
C(4A)–C(5A)–C(6A)	121.6 (4)	120.3 (2)	119.0 (3)
C(4B)–C(5B)–C(6B)	120.5 (4)		119.9 (3)
O(2A)–C(5A)–C(4A)			114.6 (3)
O(2A)–C(5A)–C(6A)			126.4 (3)
O(2B)–C(5B)–C(4B)			115.2 (3)
O(2B)–C(5B)–C(6B)			124.9 (3)
N(3)–C(5)–C(4)		119.6 (2)	
N(3)–C(5)–C(6)		120.1 (2)	
C(1A)–C(6A)–C(5A)	120.5 (4)	121.4 (2)	121.5 (3)
C(1B)–C(6B)–C(5B)	121.3 (4)		120.7 (3)
N(1A)–C(7A)–C(1A)	124.6 (3)	124.4 (1)	126.1 (3)
N(1B)–C(7B)–C(1B)	124.9 (4)		126.7 (3)
N(1A)–C(8A)–C(9A)	106.7 (3)	105.6 (1)	107.6 (3)
N(1B)–C(8B)–C(9B)	106.3 (3)		107.9 (3)
N(2A)–C(9A)–C(8A)	107.3 (3)	107.9 (1)	108.1 (3)
N(2B)–C(9B)–C(8B)	107.6 (3)		108.5 (3)
Fe–N(1B)–C(8B)	113.7 (3)	113.7 (1)	115.8 (2)
C(7A)–N(1A)–C(8A)	119.2 (3)	120.5 (1)	118.6 (3)
C(7B)–N(1B)–C(8B)	119.4 (3)		118.4 (3)
Fe–N(2A)–C(9A)	105.3 (2)	108.0 (1)	105.4 (2)
Fe–N(2B)–C(9B)			106.4 (2)
Fe–N(2A)–C(10A)	116.3 (3)		116.2 (2)
Fe–N(2B)–C(10B)			114.2 (2)
C(9A)–N(2A)–C(10A)	109.8 (3)		113.1 (3)
C(9B)–N(2B)–C(10B)	110.7 (3)		111.1 (3)
O(2)–N(3)–O(3)		122.1 (1)	
O(2)–N(3)–C(5)		119.6 (1)	
O(3)–N(3)–C(5)		118.2 (2)	
C(2A)–C(1A)–C(6A)	119.6 (4)	119.2 (2)	119.9 (3)
C(2B)–C(1B)–C(6B)	119.4 (4)		120.1 (3)
C(2A)–C(1A)–C(7A)	122.8 (3)	122.7 (1)	122.4 (3)
C(2B)–C(1B)–C(7B)	121.6 (4)		122.9 (3)
C(6A)–C(1A)–C(7A)	117.6 (4)	118.1 (1)	117.5 (3)
C(6B)–C(1B)–C(7B)	119.0 (4)		116.9 (3)
O(1A)–C(2A)–C(1A)	124.8 (3)	124.2 (1)	123.0 (3)
O(1B)–C(2B)–C(1B)	126.2 (4)		123.1 (3)
O(1A)–C(2A)–C(3A)	116.6 (3)	118.2 (1)	119.3 (3)
O(1B)–C(2B)–C(3B)	116.8 (3)		118.9 (3)
C(1A)–C(2A)–C(3A)	118.5 (3)	117.6 (2)	117.7 (3)
C(1B)–C(2B)–C(3B)	117.0 (4)		118.0 (3)

Table IV. Average Fe–Ligand Bond Distances (Å) in $[Fe^{III}(5\text{-}OCH_3Salmeen)_2]PF_6$, $[Fe^{III}(3\text{-}OCH_3Salmeen)_2]PF_6$, and $[Fe^{III}(5\text{-}NO_2Salmeen)_2]PF_6$

bond	$5\text{-}OCH_3$	$3\text{-}OCH_3$	$5\text{-}NO_2$
⟨Fe–O⟩[a]	1.914	1.879	1.886
⟨Fe–N(imino)⟩[a]	2.100	1.934	1.944
⟨Fe–N(amino)⟩[a]	2.209	2.060	2.046
⟨Fe–L⟩[b]	2.074	1.957	1.959

[a] Average of the two bond distances. [b] Average of the six Fe–ligand bond distances.

the ethylenediamine chelate ring is likely responsible for the shorter Fe–N(amino) bond distances in the hexadentates, although the additional influence of a $[N\text{–}H\cdots OH_2]$ hydrogen-bonding network, present in the low-spin $[Fe^{III}(Sal)_2trien]^+$ hexadentate complexes[9] but absent in the anhydrous $[Fe^{III}(XSalmeen)_2]PF_6$ compounds, is difficult to assess.

Regardless of exact origin, it seems significant that an identical value of $\delta_{av} = 0.12\text{–}0.13$ Å is found for both the spin-equilibrium hexadentate and bis tridentate $[Fe^{III}(Salmeen)_2]^+$ complexes, and from inspection of Table V, this δ_{av} value may indeed be quite general for molecular structural change associated with (low spin) ⇄ (high spin) transitions in $3d^5$ systems. Furthermore, the available data in the table suggests that substantially larger primary coordination sphere reorganizational processes ($\delta_{av} \simeq 0.20$ Å) may be generally characteristic of $3d^6$ spin-transition phenomena. This being the case, the result is not inconsistent with our previous suggestion[33] that intersystem crossing rates in spin-equilibrium complexes may be strongly rate determined by the extent of the structural reorganizational processes that must accompany the intersystem crossing event (some of the slowest rates have been measured for $3d^6$ systems).

Table V. Available Structural Information for Six-Coordinate $3d^5$ and $3d^6$ Spin-Equilibrium Complexes

compd	ligand dentate character, donor atom set	δ_{av},[a] Å	ref
	$3d^5$ Systems		
$[Fe^{III}(X\text{-}Salmeen)_2]^+$	tri, N_4O_2	0.12	this work
$[Fe^{III}(Sal)_2trien]^+$	hexa, N_4O_2	0.13	9
$[Fe^{III}(Acac)_2trien]^+$	hexa, N_4O_2	0.13	9
$[Fe^{III}(dtc)_3]$[b]	bi, S_6	0.11	3, 9
$[Fe^{III}(mtk)_3]$[c]	bi, S_3O_3	0.09[d]	4
	$3d^6$ Systems		
$[Fe^{II}(6\text{-}Mepy)_3tren]^{2+}$[e]	hexa, N_6	0.26[h]	5, 6, 9
$[Fe^{II}(2\text{-}pic)_3]^{2+}$[f]	bi, N_6	0.19	11
$[Fe^{II}(pyz)_2]$[g]	tri, N_6	0.20	12

[a] The average metal–ligand bond distance change estimated to occur upon total (high spin) → (low spin) conversion. [b] dtc = dithiocarbamate ligands. [c] mtk = monothio-β-diketonate ligands. [d] Lower limit. [e] $(6\text{-}Mepy)_3tren$ = the [4-(6-methyl-2,2′-bipyridyl-3-yl)-3-aza-3-butenylamine] ligand. [f] 2-pic = 2-picolylamine ligands. [g] pyz = pyrazolylborate ligands. [h] Upper limit.

Future studies of spin-state dependency on molecular structure will focus on further exploring the generality of the δ_{av} trend suggested in Table V for $3d^5$ and $3d^6$ systems (both $\Delta S = 2$ processes), as well as for $\Delta S = 1$ $3d^7$ cases where such structural information is even more critically lacking.

Acknowledgment. We gratefully acknowledge financial support by the Robert A. Welch Foundation (Grant C-627)

---

(33) See for example: Dose, E. V.; Hoselton, M. A.; Sutin, N.; Tweedle, M. F.; Wilson, L. J. *J. Am. Chem. Soc.* **1978**, *100*, 1141.

and by the National Science Foundation (Grant CHE77-14594) for work done at Rice University and the National Science Foundation (Grant CHE77-01372) for work done at the University of Virginia.

Registry No. $[Fe^{III}(3\text{-}OCH_3Salmeen)_2]PF_6$, 65293-76-7; $[Fe^{III}(5\text{-}NO_2Salmeen)_2]PF_6$, 65293-68-7; $[Fe^{III}(5\text{-}OCH_3Salmeen)_2]PF_6$, 65293-72-3.

Supplementary Material Available: Tables of hydrogen atomic parameters, bond distances and angles within the PF_6^- anions, and observed and calculated structure factor amplitudes (37 pages). Ordering information is given on any current masthead page.

Contribution from the Department of Chemistry, University of Massachusetts, Amherst, Massachusetts 01003, and the Institut für Anorganische Chemie, Universität München, D-8000 München 2, Germany

Bridgehead Phosphorane Structures in Tetrafluoro- and Tetrachlorodiazadiphosphetidines with Fused Five-Membered Rings[1,2]

ROBERTA O. DAY,[3a] ROBERT R. HOLMES,*[3a] HELMUT TAUTZ,[3b] J. HELMUT WEINMAIER,[3b] and ALFRED SCHMIDPETER*[3b]

Received July 29, 1980

P,P-Difluoro- and *P,P*-dichloro-1,3,4,2-oxadiazaphospholes and -1,2,4,3-triazaphospholes form tricyclic dimers with two phosphorane bridgeheads joined together by a diazadiphosphetidine ring. NMR data are consistent with either meridional or facial ring placement in these pentacoordinate phosphorus derivatives. Single-crystal X-ray analysis of two members, the dimeric triazaphospholes $(PhCN_3MePF_2)_2$ (**4a**) and $(PhCN_3MePCl_2)_2$ (**4b**), reveal cis-facial structures. The pentacoordinated geometry around each phosphorus center is almost exactly halfway between the idealized trigonal bipyramid and square pyramid along the Berry coordinate. **4a** crystallizes in the monoclinic space group $P2_1/n$, with $a = 11.344$ (7) Å, $b = 11.617$ (5) Å, $c = 14.254$ (11) Å, $\beta = 96.83$ (6)°, and $Z = 4$. **4b** crystallizes in the monoclinic space group $P2_1/c$ with $a = 6.585$ (2) Å, $b = 21.383$ (9) Å, $c = 15.824$ (7) Å, $\beta = 103.89$ (4)°, and $Z = 4$. Data for both compounds were collected, with an automated Enraf-Nonius CAD 4 diffractometer, out to a maximum $2\theta_{\mathrm{Mo\,K\bar{\alpha}}}$ of 50°. Full-matrix least-squares refinement techniques led to the final agreement factors of $R = 0.042$ and $R_w = 0.051$ for **4a** on the basis of 2059 reflections having $I \geq 2\sigma_I$ and $R = 0.036$ and $R_w = 0.046$ for **4b** for the 2855 reflections having $I \geq 2\sigma_I$. The cis-facial conformation for **4a** and **4b** in contrast to the meridional form found for two related tricyclic diphosphoranes is attributed to the dominance of halogen apicophilicity over the preference for nitrogen planarity. The extent of displacement toward the square pyramid is viewed as a measure of the relative importance of these two effects. A low-energy path for intramolecular ligand exchange is suggested to account for the suspected fluxional behavior indicated by the NMR data.

Introduction

Two trigonal bipyramids having a central phosphorus atom and sharing an edge between an apical and an equatorial nitrogen atom constitute the (idealized) structure of diaza-di-λ^5-phosphetidines, Ia. These dimeric phosphoranes exist when substituents of sufficient electronegativity are attached to phosphorus. For example, X-ray and in some cases electron diffraction analyses have shown the existence of this structural class for fluoro-[4-8] and chloro-substituted[9-11] derivatives. Inclusion of a second small ring, leading to the spirocyclic structure Ib, also helps to stabilize the diazadiphosphetidine ring. X-ray analysis of several members have been reported.[12-14]

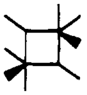

Ia

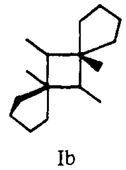

Ib

An interesting and relatively unexplored conformational problem arises if two five-membered rings are fused to the diazadiphosphetidine ring, making phosphorus (and nitrogen) bridgehead atoms. These tricyclic systems can be looked upon as dimers of five-membered cyclic phosphazenes:

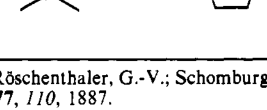

---

(1) (a) Pentacoordinated Molecules. 38. (b) Previous paper in this series: Day, R. O.; Husebye, S.; Holmes, R. R. *Inorg. Chem.* **1980**, *19*, 3616.

(2) (a) Four- and Five-Membered Phosphorus Heterocycles. 47. (b) Part 46: Schmidpeter, A.; Zeiss, W.; Schomburg, D.; Sheldrick, W. S. *Angew. Chem.* **1980**, *92*, 860; *Angew. Chem., Int. Ed. Engl.* **1980**, *19*, 825.

(3) (a) University of Massachusetts. (b) Universität München.

(4) Cox, J. W.; Corey, E. R. *Chem. Commun.* **1967**, 123.

(5) Almenningen, A.; Andersen, B.; Astrup, E. E. *Acta Chem. Scand.* **1969**, *23*, 2179.

(6) Sheldrick, W. S.; Hewson, M. J. C. *Acta Crystallogr., Sect. B* **1975**, *B31*, 1209.

(7) Fild, M.; Sheldrick, W. S.; Standiewicz, T. *Z. Anorg. Allg. Chem.* **1975**, *415*, 43.

(8) Harris, R. K.; Wazeer, M. I. M.; Schlak, O.; Schmutzler, R.; Sheldrick, W. S. *J. Chem. Soc., Dalton Trans.* **1977**, 517.

(9) Hess, H.; Forst, D. *Z. Anorg. Allg. Chem.* **1966**, *342*, 240.

(10) Hoard, L. G.; Jacobson, R. A. *J. Chem. Soc. A* **1966**, 1203.

(11) Weiss, J.; Hartmann, G. *Z. Anorg. Allg. Chem.* **1967**, *351*, 152.

(12) Gibson, J. A.; Röschenthaler, G.-V.; Schomburg, D.; Sheldrick, W. S. *Chem. Ber.* **1977**, *110*, 1887.

(13) Gilyarov, V. A.; Tikhonina, N. A.; Andrianov, V. G.; Struchkov, Yu. T.; Kabachnik, M. I. *J. Gen. Chem. USSR (Engl. Transl.)* **1978**, *48*, 670; *Zh. Obshch. Khim.* **1978**, *48*, 732.

(14) Lux, D.; Schwarz, W.; Hess, H.; Zeiss, W. *Z. Naturforsch., B* **1980**, *35B*, 269.

0020-1669/81/1320-1222$01.25/0 © 1981 American Chemical Society